155/3, 195–211., Budapest, 2025 DOI: 10.23928/foldt.kozl.2025.155.3.195

Architecture of the metamorphic Algyő High (SE Pannonian Basin) based on lithological interpretation of natural gamma-ray logs

KONDOR, Henrietta¹, Braun, Bence Ádám², M. Tóth, Tivadar¹

¹Department of Geology, University of Szeged, Egyetem st. 2, H-6722 Szeged, Hungary

²Fugro Austria GmbH, Einödstraße 13, H-8600 Bruck an der Mur, Austria

E-mail: kondor.henrietta@gmail.com (ORCID: https://orcid.org/0000-0001-5103-1083),

braunbence000@gmail.com, mtoth@geo.u-szeged.hu (ORCID: https://orcid.org/0000-0003-1012-1095)

A metamorf Algyő-hát (DK-Pannon-medence) kőzettani felépítése természetes gamma szelvények értelmezése alapján

Összefoglalás

A Pannon-medence részét képező Algyő-hát metamorf aljzata az egyik legjelentősebb szénhidrogén-rendszer részét képezi Magyarország délkeleti területén. A múlt században több mint 100 kutatófúrás érte el a terület aljzatát, melyek jelentős mennyiségű magmintát és lyukgeofizikai adatot szolgáltatnak. Jelen tanulmány során a lyukgeofizikai adatok áttekintése és elemzése lehetővé tette a fő metamorf kőzettípusok és a geofizikai mérési adatok közötti kapcsolatrendszer feltárását, ezáltal a magmintákból nyert információk térbeli kiterjesztését. A területen a geofizikai-kőzettani korrelációhoz a természetes gamma intenzitás-szelvény bizonyult a legalkalmasabbnak. Ez a szelvény különösen érzékeny az egyes kőzettípusok ásványos és kémiai összetételére, és hatékony a nagy léptékű kőzettani azonosításban. Az eredmények jelentős kőzettani eltéréseket tártak fel az aljzatban, amelyeket a gamma intenzitások változásai jellemeznek. A teljes területre vonatkozó lyukgeofizikai szelvények megerősítik az Álgyő-hát háromosztatú blokkos felépítését. A gránátos-kianitos gneisz domináns északnyugati és délkeleti terület magasabb gamma intenzitással jellemezhető, mint a kis fokú kőzetekből álló központi terület, ahol alacsony gamma intenzitások tapasztalhatók. A teljes terület elemzése a délkeleti területen magas gamma intenzitású anomáliákat tárt fel. A petrográfiai és lyukgeofizikai adatok alapján a délkeleti terület fő kőzettípusa a gránátos–kianitos gneisz, amelyben alacsony gamma intenzitással jellemezhető gránátos amfibolitzónák is azonosíthatók. A gneisztömegen belül magasabb gamma intenzitással rendelkező metagránit jelentkezett. E kőzet a gneiszbe nyomult fiatal gránit/granodiorit intrúziós telérekként értelmezhető, amelyek jelentős hatást gyakorolhattak a befogadó gneisz ásványos és kémiai összetételére. Ennek eredményeként a gránátos-kianitos gneiszben metaszomatizált zónák alakultak ki, amelyek metaszomatizált gneiszként kerültek elkülönítésre. A lyukgeofizikai adatok és magminták együttes értelmezése nagymértékben hozzájárult a terület komplex kőzettani felépítésének és szerkezetfejlődésének megértéséhez.

Tárgyszavak: Algyő-hát, lyukgeofizika, természetes gamma szelvény, kőzettani azonosítás

Abstract

The metamorphic basement of the Algyő High, located in the Pannonian Basin, is a reservoir unit within an important hydrocarbon system in the SE part of Hungary. Over the past century, more than 100 exploration wells have reached the basement in the area, providing a substantial number of core samples and well-log data for analysis. This study reviewed and analysed well-log data from these boreholes to establish correlations between primary metamorphic rock types and wireline logs, enhancing the spatial information derived from core samples. For geophysical-lithological correlation, natural gammaray intensity logs were considered the most suitable for this area. These logs are sensitive to lithological variations and are effective for large-scale lithological identification. Our results reveal significant lithological variations within the basement, reflected in variations in gamma-ray intensities. The well-log data for the entire area confirm that the basement of the Algyő High comprises three major blocks. The northwest and southeast portions of the area, dominated by garnet-kyanite gneiss, exhibit higher gamma intensities compared to the central region, which is characterised by low-grade metamorphic rocks and lower gamma intensities. The analysis of the entire region revealed anomalies in gamma intensities in the southeastern part. Focusing on this area, the petrographic and well-log data indicated that the basement is dominated by garnet–kyanite gneiss with zones of garnetiferous amphibolite with low gamma intensities. Within the gneiss mass, metagranite with higher gamma intensities was identified. This rock type is interpreted as young granite/granodiorite intrusive dykes. These intrusions may have affected the mineralogical and chemical composition of the host gneiss, resulting in metasomatised zones within the garnet-kyanite gneiss realm, which are interpreted as metasomatised gneiss. The analysis of wireline data in conjunction with core samples provides new insights into the complex lithological composition and structural evolution of the area.

 $Keywords: Algy\'{o}\ High,\ well-logging,\ natural\ gamma\ logs,\ lithology\ identification$

Introduction

The crystalline basement of the Pannonian Basin exhibits a complex geological structure. Previous studies have demonstrated that the Variscan basement comprises blocks with distinct metamorphic histories, resulting from multiphase tectonic evolution from the Mesozoic to the Neogene. During the later stages of Neogene basin evolution, uniform subsidence led to the burial of these fault-segmented crystalline basement blocks beneath thick sedimentary sequences. While these Neogene sediments have proven to be important hydrocarbon reservoirs, recent research has emphasised the critical role of the basement in fluid storage and migration (SCHUBERT et al. 2007, M. TÓTH 2008, NAGY et al. 2013, Molnár et al. 2015, M. Tóth & Vargáné Tóth 2020, M. Тотн et al. 2021). This highlights the importance of gaining a comprehensive understanding of the geological characteristics and structural evolution of the crystalline basement.

Investigations into these metamorphic formations are typically conducted using drill cores and well-logging. Although core samples provide detailed lithological information, their spatial coverage is restricted to a narrow zone surrounding the borehole. In contrast, geophysical measurements, such as wireline logging, allow for the continuous characterisation of the entire rock column penetrated by the well, thereby expanding the lithological information. In recent decades, well-logging has become a highly advanced tool in sedimentology, and it is used to determine lithology, fluid content, and various petrophysical properties. More recently, wireline logs have also been applied to characterise mineralogically and structurally complex igneous and metamorphic rock bodies (BARTETZKO et al. 2005, PECHNIG et al. 2005, Fiser-Nagy et al. 2014, Molnár et al. 2015, M. Tóth & VARGÁNÉ TÓTH 2020, HASAN & M. TÓTH 2023). The Algyő High, located in the central part of Hungary's main hydrocarbon system, represents a key example (MAGYAR et al. 2006). Its basement has been penetrated by over 100 exploration wells over the past century; however, these predominantly reached only the uppermost part of the metamorphic basement. Consequently, although lateral lithological correlations can be established, the deeper levels remain unexplored. In a previous study, KONDOR & M. TÓTH (2021) characterised and classified the principal rock types of the Algyő High. Through comprehensive petrographic analyses of drill cores, they identified distinct metamorphic histories and spatial relationships between these rock types.

The present study aims to establish correlations between primary metamorphic rock types and wireline logs, enhancing and expanding the spatial information derived from core samples. In this study, all available well-log data were reviewed and analysed, and the most suitable methods for the area were applied. This integrated approach significantly improved the understanding of the lithological composition and structural framework of the region. Furthermore, the lithological characteristics of the SE part of the Algyő High were re-evaluated as part of this interpretation.

Geological setting

The basement of the Tisza–Dacia Mega-unit, located in the Pannonian Basin, comprises Variscan rocks with varied metamorphic histories. During the Lower Cretaceous compression phase, the Tisza–Dacia Mega-unit was divided into four NW-facing nappes: the Mecsek, Villány–Bihor, Békés–Codru, and Biharia Nappe Systems (HAAS 2001, Csontos & Vörös 2004). Geophysical interpretations suggest that the Middle Miocene syn-rift extension initiated lowangle normal fault systems, forming asymmetric half-graben structures and exposing metamorphic core complexes (Tari et al. 1992, Tari 1996). The subsequent post-rift thermal sag and compressional phase reactivated these normal faults, leading to the uplift of metamorphic highs.

The Algyő High (AH) is an elevated, NW–SE-oriented metamorphic dome located approximately 2.5–3.0 km below the present surface in southeastern Hungary. Miocene faults bound this basement high, separating it from the Makó Trough to the east and the Szeged Basin to the west (*Figure 1*).

Previous studies indicate that the basement of the AH primarily consists of gneiss, mica schist, chlorite schist, and epidote-bearing rocks. Additionally, the host gneisses contain amphibolite lenses and pegmatite and aplite dykes associated with felsic magmatism (Juhász 1969, Szalay 1977, Szederkényi 1984, T. Kovács & Kurucz 1984, Kondor & M. Tóth 2021). Szalay (1977) identified the young granite bodies within a narrow zone of the Variscan crystalline formations, interpreting them as having formed during a post-peak-metamorphic event. T. Kovács & Kurucz (1984) described mylonitic granite bodies in the southeastern AH, which Szederkényi (1984) referred to as the Deszk Migmatite Formation, associating them with a possibly Late Cretaceous magmatic event.

According to a comprehensive petrological study by KONDOR & M. TÓTH (2021), the AH area consists of blocks with distinct metamorphic histories. They proposed that the northwestern and southeastern parts of the region predominantly consist of garnet–kyanite gneiss associated with garnetiferous amphibolite, interpreted as disaggregated blocks of the same rock body. The central part of the region is characterised by well-defined segments of epidote orthogneiss and chlorite schist (*Figure 2*).

According to previous publications, the gneiss rocks were affected by polyphase metamorphism (Szalay 1977; Szederkényi 1984; T. Kovács & Kurucz 1984; Horváth & Árkai 2002; Lelkes-Felvári et al. 2003, 2005; Kondor & M. Tóth 2021). Lelkes-Felvári et al. (2003, 2005) proposed that the rocks were subjected to an early high-temperature/low-pressure metamorphism, forming andalusite. Based on this model, the first metamorphic event was overprinted under amphibolite facies conditions, during which the early andalusite transformed into kyanite. Based on thermobarometric calculations by Horváth & Árkai (2002), the first metamorphic event (M1) affecting the garnet–kyanite gneiss is characterised by staurolite appearance at 520–

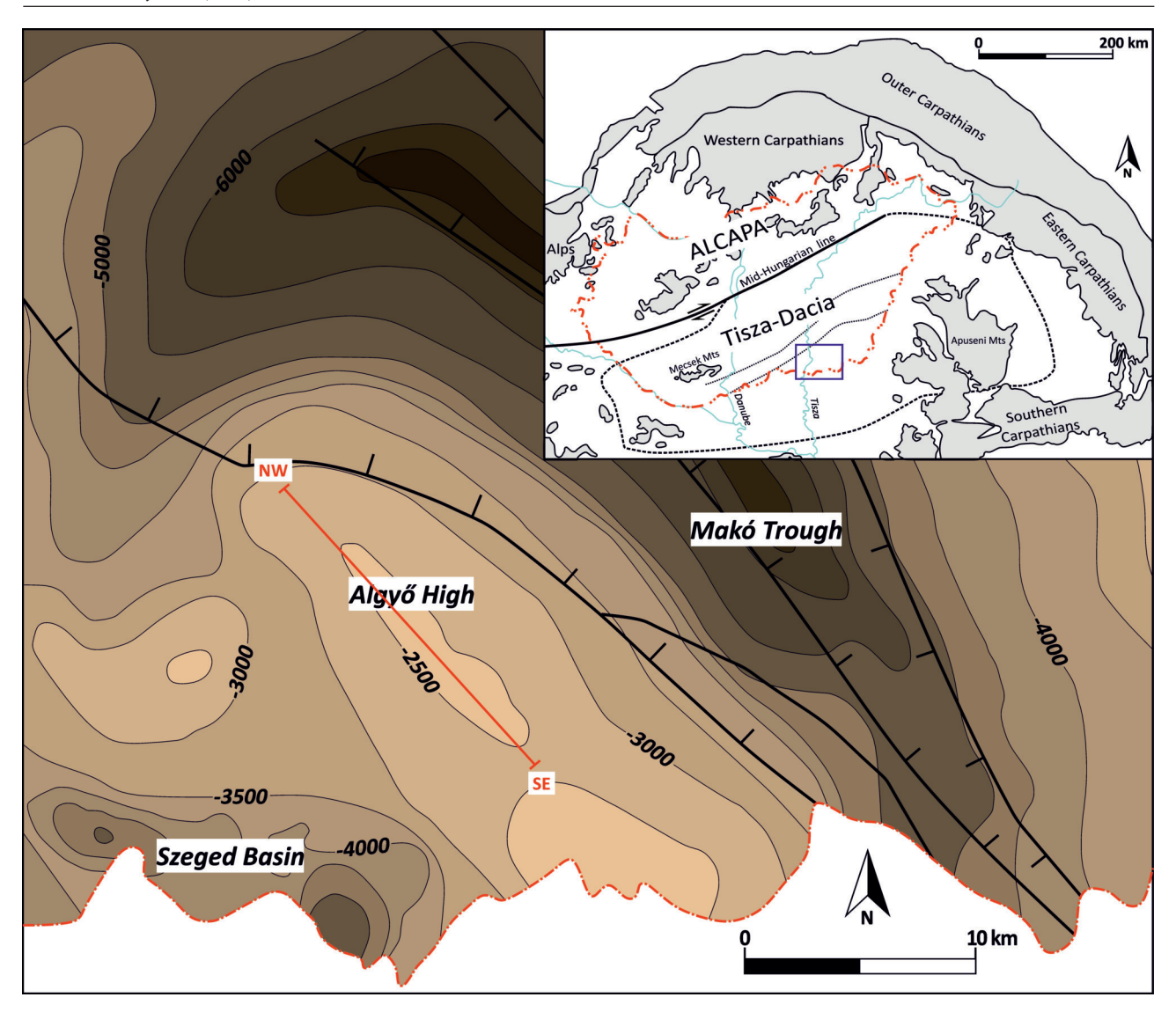


Figure 1. Location of the Algyő High and the surrounding pre-Cenozoic basement (modified after Haas et al. 2010) inside the Carpathian-Pannonian region (after Csontos et al. 1992). The NW-SE line indicates the location of the geological cross-section shown in Figure 2.

1. ábra. Az Algyő-hát és környezetének prekainozoos alaphegységi helyzete (HAAS et al. 2010 után módosítva) a Kárpát-Pannon régióban (Csontos et al. 1992 után módosítva). A piros vonal a 2. ábrán bemutatott földtani szelvény nyomvonalát jelöli

560 °C and 820–1010 MPa. The second event (M2) yielded peak conditions of 650-680 °C and 500-600 MPa, which resulted in kyanite formation replacing staurolite. Based on TWQ modelling, KONDOR & M. TÓTH (2021) proposed the second event was a contact metamorphic (metasomatic) process linked to an igneous intrusion. During this process, finegrained kyanite aggregates formed at the expense of garnet. They consider the presence of post-kinematic tourmaline in a gneiss terrane as further evidence of the contact overprint. Based on garnet Sm-Nd data, Lelkes-Felvári et al. (2003) determined the first metamorphic event to be Permian in age (273±7 Ma). The second event, confirmed through Ar-Ar plateau ages on secondary muscovite crystals, as a Late Cretaceous, eo-Alpine regional metamorphic overprint, established at 82-95 Ma (Lelkes-Felvári et al. 2003) and 68.4-84.3 Ma (BALOGH & PÉCSKAY 2001).

The central part of the AH consists of chlorite schist and epidote orthogneiss, which are characterised by markedly different metamorphic evolutions compared to the polymetamorphic gneiss domain (Szalay 1977, T. Kovács & Kurucz 1984, Kondor & M. Tóth 2021). The microtextural features of the epidote orthogneiss suggest an intrusive granitoid protolith with greenschist facies (~400 °C) retrograde metamorphism. In contrast, the chlorite schist underwent metamorphism along a low-grade progressive pathway. The peak conditions are estimated to have been in the chlorite-biotite zone, followed by a post-metamorphic, metasomatic overprint (Kondor & M. Tóth 2021). Based on the suggested metamorphic evolution of these two low-grade rocks, they are interpreted as two distinct blocks with different metamorphic histories (Kondor & M. Tóth 2021).

The Cretaceous compressional phase in this region resulted in the formation of nappe systems in both the Mesozoic cover formations and the Variscan crystalline basement (Tari et al. 1999, 2003). According to the current model, the structural build-up of the adjacent Dorozsma High (DH)

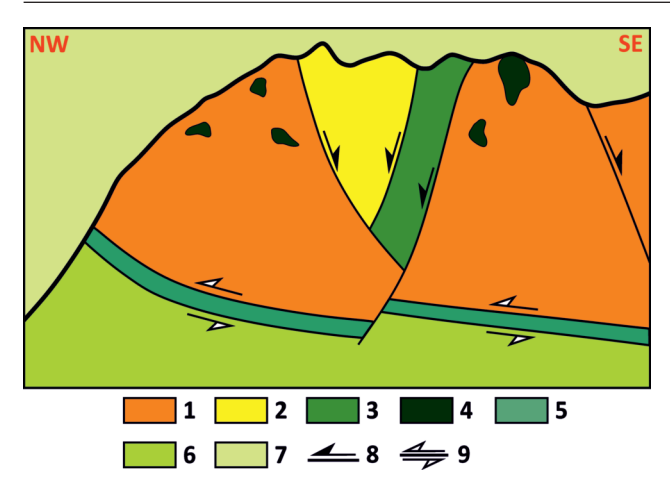


Figure 2. Schematic geological structure of the Algyő High (modified after Kondor & M. Tóth 2021). The location of the NW-SE cross-section is shown in Figure 1. (1) garnet-kyanite gneiss, (2) epidote orthogneiss, (3) chlorite schist, (4) garnetiferous amphibolite, (5) dolomite marble, (6) amphibolite-dominated block, (7) Neogene sediments, (8) Miocene normal faults, (9) Aldine thrust sheet

2. ábra. Az Algyő-hát sematikus geológiai szerkezete (KONDOR & M. TÓTH 2021 után módosítva). A NW-SE szelvény nyomvonalát az 1. ábra jelöli. (1) gránátos-kianitos gneisz, (2) epidotos ortogneisz, (3) kloritpala, (4) gránátos amfibolit, (5) dolomitmárvány, (6) amfibolit-domináns blokk, (7) neogén üledékek, (8) miocén normál vetők, (9) alpi takaró határ

was formed due to this event. Here, from top to bottom, garnet–kyanite gneiss, dolomite marble, and an amphibolite-dominated rock body characterise the basement, where the intensively deformed dolomite marble cataclasite zone is interpreted as a large-scale, Early Cretaceous nappe border (M. TÓTH 2008, M. TÓTH & VARGÁNÉ TÓTH 2020). Considering the petrological similarities between the garnet–kyanite gneiss of AH and DH, KONDOR & M. TÓTH (2021) suggest a three-part structure for the AH similar to that of the DH, implying an Alpine thrust sheet beneath the garnet–kyanite gneiss block (*Figure* 2).

Previous studies showed that, during the Late Cretaceous, the entire region was subject to intrusion by granite/granodiorite ('banatite') bodies (Szederkényi 1984, Berza et al. 1998, Neubauer 2002, Zimmerman et al. 2008, Reiser 2015). SZEDERKÉNYI (1984) suggests that the young dykes within the gneiss body, the crystallisation of tourmaline and secondary muscovite, the polymetallic sulphide mineralisation, as well as the positive Mo, Sn and W anomaly, are all linked to 'banatite' magmatism. Earlier studies also evaluate the granite bodies in the SE part of AH as young intrusions (SZALAY 1977, T. KOVÁCS & KURUCZ 1984). KONDOR & M. Тотн (2021) interpret the tourmaline crystallisation documented in the garnet-kyanite gneiss and the metasomatic overprint of the chlorite schist as being connected to the hydrothermal overprint of these granite intrusions. However, no age data regarding these intrusions are available at present.

The AH has a metamorphic core complex structure (TARI et al. 1999) formed by Middle Miocene syn-rift extensional processes (RUMPLER & HORVÁTH 1988, POSGAY et al. 1996). During this phase, blocks with different metamorphic histories were probably juxtaposed along post-metamorphic

normal faults (Kondor & M. Tóth 2021) (*Figure 2*). This stage was followed by a post-rift thermal sag phase, during which the entire region became covered by thick Neogene sediments (Horváth & Tari 1999), hosting large amounts of hydrocarbon. Based on analogues, the brittle fault zones between the blocks with differing metamorphic evolution in the AH area may play an essential role in fluid migration from the adjacent deep sub-basins or could even act as reservoirs (Kondor & M. Tóth 2021).

Data availability

Open-hole well logs

A total of 102 boreholes have penetrated the basement of the AH area. Out of these wells, only 66 have well-log data available, with core samples accessible from 41. In the case of 19 wells, neither core samples nor well-logs are available (*Figure 3*).

The available wireline geophysical data are derived from two distinct technological eras:

i) The older logs, dating back to the 1960s and early 1970s, originated from the early days of hydrocarbon exploration in the area. Core sampling was typically performed during this period, as the boreholes served exploratory purpose.

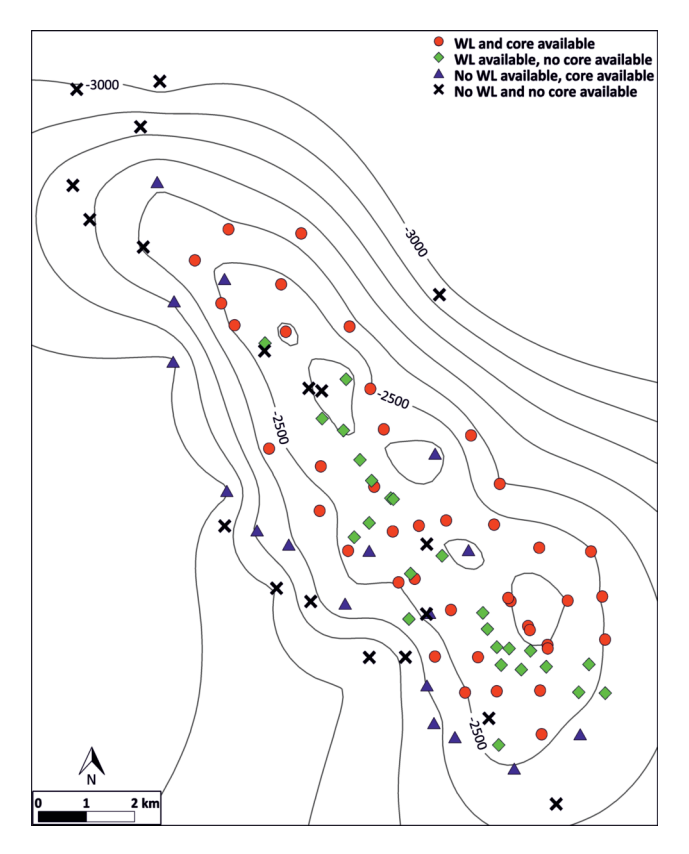


Figure 3. Point map showing the availability of drillcores and well-logs (WL) from the Algyő High area

3. ábra. Az Algyő-hát területéről származó fúrómagok és lyukgeofiziai adatok elérhetőségének ponttérképe

ii) The more modern logs come from the late 1970s and early 1980s. During this period, core sampling was not performed as these wells were drilled for hydrocarbon production.

In the case of the older types of well-logs, data include natural gamma-ray intensity (NGR [CGU]), neutron gamma (NGPOR [CNU]), spontaneous potential (SP [mv]), microlog potential and microlog gradient (RESMP and RESMG [ohmm]). According to the drilling completion reports, resistivity measurements were conducted in many boreholes using conventional Soviet BKZ tools. However, the well-log data were not accessible in these instances. Data included in the newer types of logs comprise natural gamma-ray intensity (NGR [API], neutron porosity [NNPOR [V/V%]), rock density (RHOB [g/cm³]), acoustic travel time (AT [μs/ft]) and microlaterolog resistivity (RESMLL [ohmm]).

Given the availability of wireline data associated with core sampling information, their applicability in a metamorphic formation, as well as the reliability of calibrations and measurements, the NGR [CGU] well-log is considered the most suitable for geological—geophysical investigations in this area. Among the available logging methods, NGR is the most sensitive to the mineralogical and chemical composition of rocks, which is essential for distinguishing between different types of metamorphic rocks. This log is particularly effective for large-scale lithological identification and provides comprehensive geological correlation and data enhancement coverage.

Natural gamma-ray log interpretation

The measurement of natural gamma-ray intensity is based on the detection of radiation from the natural decay of radioactive isotopes within the formations. Gamma activity is primarily controlled by the type and quantity of radioactive elements and rock density. The most common sources of gamma radiation are potassium (40K), thorium (232Th), and uranium (238U) (SERRA 1984). This method is widely used in sedimentology, and is also applicable to distinguish igneous and metamorphic rock types (PECHNIG et al. 2005, BARTETZKO et al. 2005, Luo & Pan 2010). The level of emitted gamma radiation strongly depends on mineralogical and chemical composition. Rocks rich in K-feldspar, biotite, muscovite, or clay minerals (e.g., illite) show increased gamma activity. In felsic igneous rocks and orthogneisses, gamma intensity is mainly influenced by K-feldspar content, whereas in paragneisses and some mafic rocks, it is influenced by biotite and white mica content (PECHNIG et al. 2005). In igneous rocks, potassium and uranium content have a particularly strong impact on gamma emission, with felsic magmatites typically showing higher uranium content than mafic rocks (Larsen et al. 1954). According to Bartetzko et al. (2005), elevated NGR values in metamorphic rocks may also reflect metasomatic or hydrothermal overprinting.

For NGR logs, two datasets with different calibrations are available. In most boreholes, measurements were expressed in Conditional Gamma Units [CGU] using early-

generation tools. As only a small number of wells include measurements in standardized American Petroleum Institute [API] units, and no borehole contains NGR data in both API and CGU formats – with the necessary standardization coefficients unknown - no reliable correlation can be established between the two log types. In earlier gamma-ray logging practices, the CGU scale was developed as a localized, project-specific standard rather than a universal API-based one. The process began with the identification of reference intervals. These zones were confirmed through lithological descriptions or core analyses. These reference layers served as calibration points for the natural gamma-ray logs. An empirical relationship was then established between NGR values and clay content (in reality potassium (40K) and/or thorium (232Th), and uranium (238U), derived from the reference intervals. Based on this relationship, a conditional CGU scale was defined for the study area, translating NGR values into corresponding lithologies. Once established using selected reference boreholes, this CGU scale was applied to other wells in the same area. It is important to note that early gamma-ray tools were not API-standardized, lacked consistent calibration blocks, and had varying sensitivities. Consequently, the CGU logs provide primarily qualitative insights and were not intended to represent absolute radioactivity; rather, they served as a relative, lithology-oriented classification based on inferred natural radioactive-element content.

Core samples and thin sections

In a previous study, KONDOR & M. TÓTH (2021) characterised and classified the principal rock types of the AH area, each with a distinct metamorphic history, based on comprehensive petrographic analyses of drill cores. Based on these previous results, the petrographic features of the SE part of the AH were characterised and specified by reanalysing available core samples. In this region, 36 boreholes reached the metamorphic basement, and core samples for petrographic analysis were obtained from 21 of these. A total of 46 thin sections were reanalysed from these cores, typically two or more per borehole. The aim of the petrographic characterisation was to determine the mineralogical composition, microtexture, and microstructure of each rock type, which served as a basis for reconstructing their qualitative metamorphic evolution. The thin sections were analysed using an Olympus BX41 polarisation microscope.

Methodology

Although multivariate statistical analyses, particularly discriminant analysis, have been widely applied in recent years to differentiate metamorphic rocks based on their well-log responses (FISER-NAGY et al. 2014, MOLNÁR et al. 2015a, HASAN & M. TÓTH 2023), its applicability in this area is quite limited. Using all available NGR [CGU] data, a large-scale, 3D block model of the entire AH region was created in RockWorks15 modelling software with a voxel resolution of

25×25×1 metres. A representative cross-section, illustrating the main structural features of the entire area, was derived from the 3D model. The interpretation of this dataset is based on the petrological results of KONDOR & M. TÓTH (2021). The resulting map allows the identification of largescale lithological variations and potential anomalies. Focusing on the SE part of the area, a more detailed 3D block model was constructed from the NGR [CGU] dataset, with a voxel resolution of 8×8×0.8 metres, using the same software. This provided enhanced insights into the geological structures of the area. Based on the interpolated model, crosssections were generated in multiple directions, covering the entire SE part of the AH. Following this, the available thin sections were reanalysed, resulting in a refined and expanded petrographic characterisation of this region. The primary rock types could be identified by analysing core samples and thin sections. These results enable the correlation of petrographic and wireline log data, facilitating the reconstruction of the internal structure of the basement in the SE part.

In both 3D modelling scenarios, the anisotropic Inverse Distance Weighted (IDW) method was used as the interpolation algorithm. According to the fundamental principle of IDW, the influence of known data points decreases with distance from the prediction point, meaning that closer points have a greater impact on the interpolated value. The anisotropic IDW modelling, a specific application of the IDW method, involves the software searching for the nearest control point within each 90-degree sector, also known as an octant, around the node. The distance weight function was consistently set to a power of 2.

Only drill cores that could be clearly identified and classified through petrographic analysis were selected to establish correlations between metamorphic rock types and welllogs. By comparing the results from these core sample analyses with the NGR [CGU] logs, it was possible to ascertain the quasi-characteristic CGU values for the specific rock types. This correlation between geophysical and petrological data allows for the identification of the entire metamorphic rock column, even in boreholes lacking lithological data, and reveals spatial relationships among different rock types.

Results

General NGR characteristics of the AH area

The NW–SE oriented profile of the AH represents the distribution of average NGR [CGU] values based on the 3D model of the entire area (*Figure 4*). Along the profile, no significant vertical variations are observed; changes in natural gamma-ray intensity are primarily studied horizontally. Based on the map, data from the NW and SE parts can be compared with good approximation, showing average NGR values between 8 and 16 CGU. Exceptionally high gamma intensities (20–30 CGU) can be observed in a well located in the SE part of the area. No similar anomalies are observed in any other parts of the area. In contrast, lower values dominate the central part of the AH, typically ranging from 4 to 8 CGU, enclosed by zones with decreasing intensity towards the NW and SE directions, with values ranging from 2 to 4 CGU.

General NGR characteristics of the SE part of AH

Six profiles were generated for the SE part of the AH based on the 3D model (Figure 5). Cross-sections along these profiles reveal the general distribution of NGR [CGU] values measured in the boreholes. Where available, rock types identified from core samples were also indicated in the drill-logs. Boreholes without core sampling were marked in black (Figure 6).

Due to the shallow depth of the wells, the study of lithological changes in the vertical direction could only be conducted to a very limited extent. The comparison of natural gamma intensities is primarily feasible horizontally. Based on the obtained results, the NGR [CGU] wireline data in the area are generally characterised by values between 10 and 16 CGU, with small zones of lower values (e.g., 6–10 CGU in Well-6) can also be observed in a few wells. In some wells, natural gamma intensities are above average, ranging from 16 to 22 CGU. A significantly high gamma intensity (CGU > 22) was recorded in the Well-4.

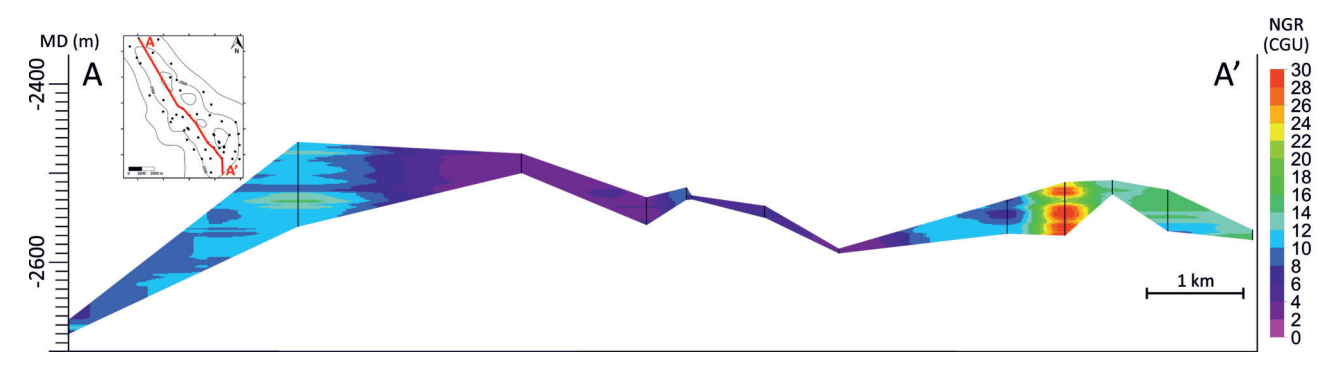


Figure 4. NW-SE cross-section across the Algyő High displaying the distribution of natural gamma-ray intensity (NGR) [Conditional Gamma Units (CGU)] values. Black lines indicate the locations of boreholes. The point map of the area illustrates the A-A' cross-section line and the wells with NGR [CGU] data. The vertical scale of the cross-section is exaggerated 2×. MD: measured depth

4. ábra. A természetes gamma intenzitás (natural gamma-ray intensity: NGR) [Feltételes Gamma Egység (Conditional Gamma Units: CGU)] értékek eloszlását mutató ÉNy-DK irányú szelvény az Algyő-hát területén. A fekete vonalak a fúrások helyét jelölik. A terület ponttérképe az A-A' szelvény nyomvonalát és az adatokat szolgáltató fúrási pontok helyét jelöli. A szelvény függőleges méretaránya kétszeres nagyítású. Az 'MD: measured depth' a mért mélységet jelöli

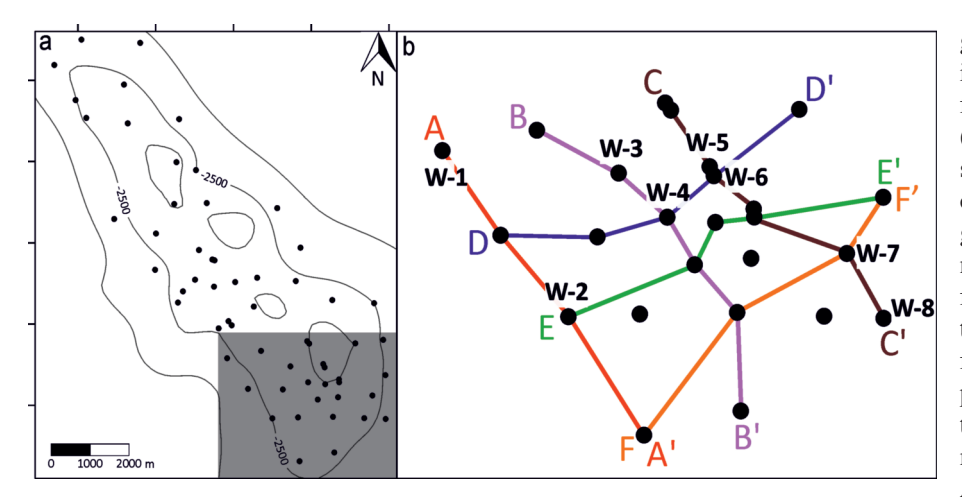


Figure 5. a) Point map displaying the well locations with natural gamma-ray intensity (NGR) data [Conditional Gamma Units (CGU)]. The grey square marks the studied SE part of the area. b) Point map showing the lines of cross-sections.

5. ábra. a) A természetes gamma intenzitás (natural gamma-ray intensity: NGR) adatokat [Feltételes Gamma Egység (Conditional Gamma Units: CGU)] szolgáltató fűrásokat jelölő ponttérkép. A szürke négyzet a vizsgált DK-i területrészt jelöli. b) A metszetek nyomvonalait jelölő ponttérkép.

Petrographic characteristics of the SE part of AH

In their previous work, KONDOR & M. TÓTH (2021) identified two main rock types in the SE part of the AH area: garnet–kyanite gneiss and garnetiferous amphibolite. The petrographic characteristics of these rocks are briefly described based on their analysis. In addition, the characteristics of the newly identified metagranite are described in detail.

The garnet–kyanite gneiss primarily consists of quartz, potassium feldspar, biotite and muscovite, with garnet porphyroblasts and fine-grained kyanite aggregates. Rutile, ilmenite, and zircon are accessory phases. In some samples, undeformed and unoriented tourmaline crystals are also present. The main foliation is defined by bands rich in biotite and muscovite and bands containing elongated quartz and feldspar grains (*Figure 7 a*). Garnet porphyroblasts appear as large, slightly elongated grains alongside small, idioblastic garnet grains. Fine-grained kyanite aggregates typically replace garnet blasts or align parallel to the foliation planes (*Figure 7 a, b*). S–C fabrics, mica fishes, and feldspar σ -clasts were also observed. Chloritisation of biotite and garnet, and sericitisation of feldspar grains are typical alterations.

The garnetiferous amphibolite is slightly oriented and characterised by nematoblastic/poikiloblastic textures. The rock-forming minerals are green or dark brown prismatic amphibole crystals, and inclusion-rich, resorbed garnet porphyroblasts. Less frequent phases included quartz, plagioclase feldspar and biotite ($Figure\ 7\ c,\ d$). Accessory minerals are rutile and titanite. The foliation plane is defined by the oriented amphibole and biotite grains ($Figure\ 7\ c$).

The main mineral phases of metagranite are potassium feldspar, plagioclase feldspar, quartz, muscovite, sericite, and subordinately biotite. Zircon, apatite, and garnet are accessory phases. The rock has an equigranular texture and is slightly foliated, defined by sericite bands, oriented muscovite and biotite flakes, and elongated quartz and feldspar

grains (Figure 7e). Large, tabular, idiomorphic or hypidiomorphic feldspar crystals with polygonal (120°) textures are frequently observed (Figure 7 f). Based on the optical properties of feldspar grains, potassium feldspar dominates the rock, while plagioclase feldspar is present in smaller quantities. Sericitisation of potassium feldspar is characteristic, while plagioclase feldspar can be identified as polysynthetic twins or myrmekitic grains (Figure 7 f, g). Additionally, microcline crystals with perthitic texture are common. Quartz grains are typically recrystallised and sub-grained. Zircon can be observed as idiomorphic crystals. In some samples, the rock is intensively deformed; mica

fishes and feldspar σ -clasts are present (*Figure 7 h*).

Discussion

Geological interpretation of the NGR characteristics of the AH area

The comprehensive petrological study of KONDOR & M. TÓTH (2021) revealed that the crystalline basement of the AH region consists of blocks with diverse metamorphic histories juxtaposed along post-metamorphic structural boundaries. This segmented structure is further evidenced by the large-scale NW-SE oriented geophysical cross-section derived from wireline data (Figure 8 a). The NW and SE parts of the area are predominantly composed of medium-grade garnet-kyanite gneiss (KONDOR & M. TÓTH 2021). By analysing well-log data from these two areas, the two petrographically similar blocks can be compared with good approximation, except for a high-value anomaly observed in one borehole in the SE part. The average NGR values in these regions range between 8-16 CGU, corresponding to the medium-grade garnet-kyanite gneiss-dominated block (Figure 8 b). The similarities in NGR characteristics confirm that the NW and SE parts of the area represent disaggregated blocks of the same rock body.

In contrast, the central region has significantly lower NGR values than the NW and SE parts. According to Kondor & M. Tóth (2021), this central area consists of a low-grade epidote orthogneiss block with a well-defined chlorite schist zone to the SE (*Figure 2*). Due to the differences in petrographic features and metamorphic evolution, these rock types are assumed to be separated by post-metamorphic structural boundaries. Based on the geophysical cross-section (*Figure 8 a*), the centre of the area is characterised by slightly higher values (4–8 CGU), which are surrounded by

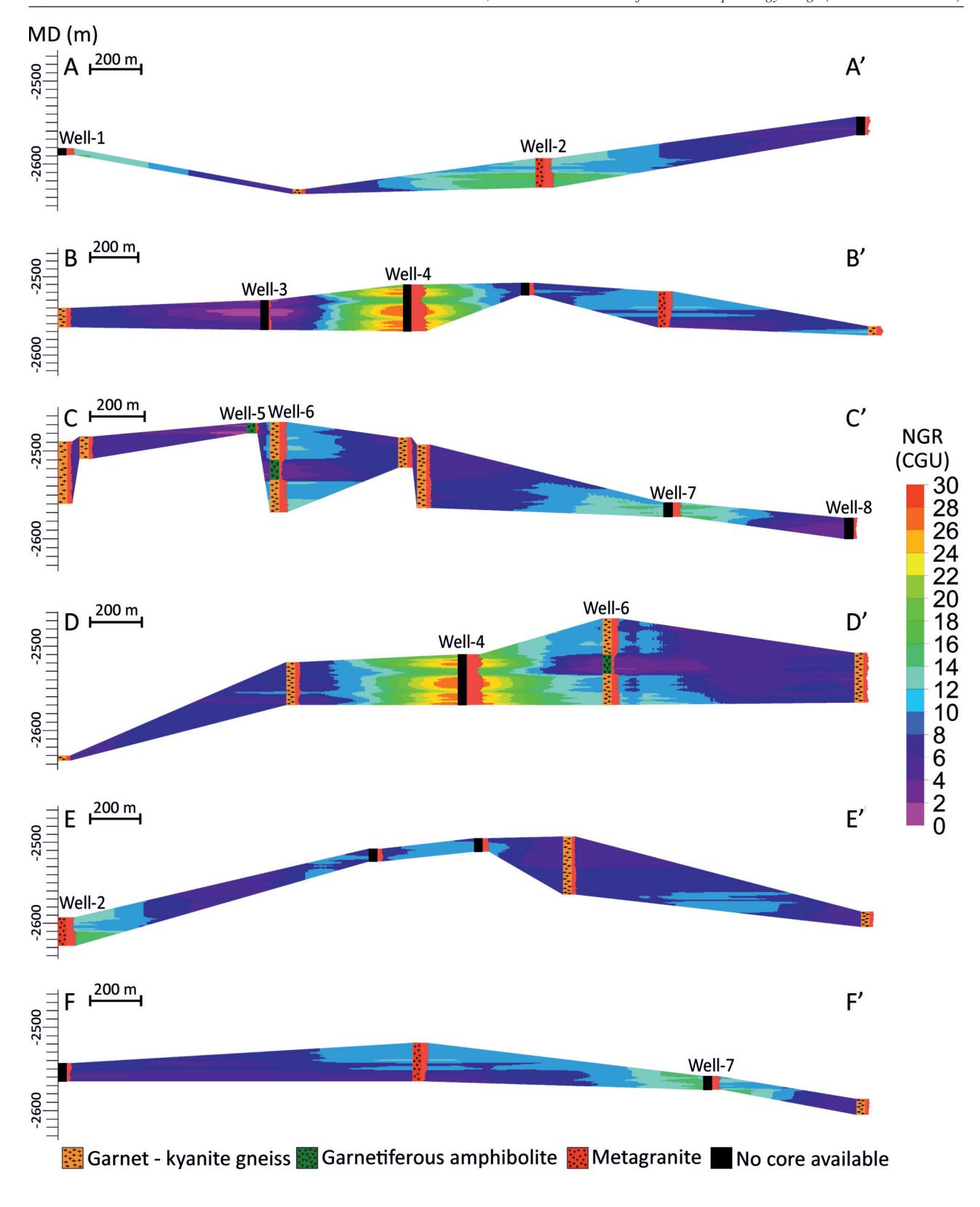
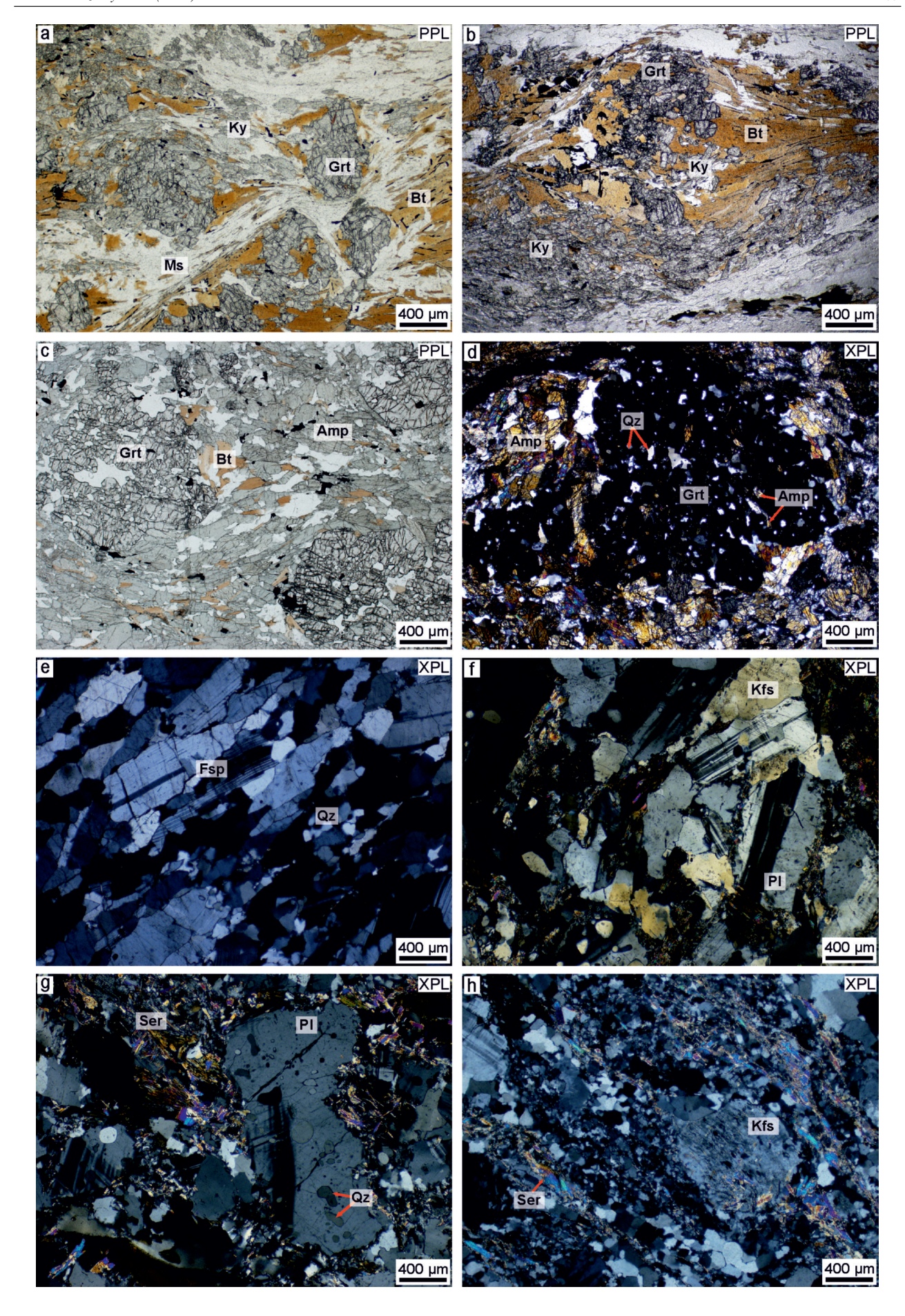


Figure 6. Cross-sections across the SE part of Algyő High illustrate the distribution of natural gamma-ray intensity (NGR) values [Conditional Gamma Units (CGU)] measured in boreholes. The rock types identified from the available core samples are marked along the boreholes. Boreholes without core samples are marked in black. The vertical scale of the cross-section is exaggerated 2×. MD: measured depth

6. ábra. Az Algyő-hát DK-i területén mélyült fúrásokban mért természetes gamma intenzitás (natural gamma-ray intensity: NGR) [Feltételes Gamma Egység (Conditional Gamma Units: CGU)] értékek eloszlását ábrázoló szelvények. A fúrások mentén a fúrásból elérhető magminták alapján azonosított közettípusok kerültek feltüntetésre. A szelvény függőleges méretaránya kétszeres nagyítású. Az 'MD: measured depth' a mért mélységet jelöli



← Figure 7. Petrographic features of the main rock types. a-b) Typical textures of garnet-kyanite gneiss. a) Muscovite and biotite bands define the foliation, with kyanite aggregates replacing garnet porphyroblasts. b) Kyanite aggregates along biotite bands parallel to foliation planes. c-d) Typical textures of garnetiferous amphibolite. c) Oriented amphibole and biotite crystals, and resorbed garnet porphyroblasts. d) Inclusion-rich garnet blast. e-h) Typical textures of metagranite. e) Elongated quartz and feldspar crystals define the foliation. f) Plagioclase twins in polygonal texture. g) Myrmekitic feldspar grain. h) Deformed feldspar σ-clast and sericite bands. PPL: plane polarised light, XPL: crossed polarised light. Mineral abbreviation after Whitney & Evans (2010)

← 7. ábra. A fő kőzettípusok petrográfiai jellemzői. a-b) A gránátos—kianitos gneisz jellegzetes szöveti jellemzői. a) Foliációt jelölő muszkovit- és biotitsávok, valamint gránát porfíroblasztokat helyettesítő kianit aggregátumok. b) A biotitos szalagok mentén, foliációs síkokkal párhuzamosan orientálódó kianit aggregátumok. c-d) A gránátos amfibolit jellegzetes szöveti jellemzői. c) Irányított amfibol- és biotitkristályok rezorbeált gránát porfíroblasztokkal. d) Zárványokban gazdag gránátblaszt. e-h) A metagránit jellegzetes szöveti jellemzői. e) A foliációt jelölő, nyúlt kvarc- és földpátkristályok. f) Poligonális szövetű plagioklász-ikerkristályok. g) Mirmekites földpátszemcse. h) Deformált földpát σ-klaszt és szericites szalagok. PPL: 1N, XPL: +N. Ásványi rövidítések Whitney & Evans (2010) alapján

zones of decreasing gamma-ray intensities (2–4 CGU) in both the SE and NW directions. In the SE part, chlorite schist is associated with gamma values of both 2–4 CGU and 4–8 CGU, based on core samples. Similarly, in the NW direction, epidote orthogneiss is linked to gamma values of 2–4 CGU and 4–8 CGU. Considering the geophysical–petrographic correlations, the low-grade metamorphic rocks in the central region cannot be distinguished based on their gamma intensities, which can be associated with their similar chemical composition. Based on the detailed petrographic description by KONDOR & M. TÓTH (2021), the rock-forming minerals of chlorite schist are quartz and chlorite, while epidote orthogneiss is primarily composed of quartz, plagioclase

feldspar, muscovite, and chloritised biotite. Additionally, significant amounts of epidote and clinozoisite have formed in the rock due to the retrograde alteration of plagioclase feldspar. In both rock types, the rock-forming minerals are potassium-free, which may explain the low gamma intensities.

The results of the NGR [CGU] well-log analyses for the entire area confirm that the basement of the AH region is composed of blocks with different petrographic characteristics. Significantly different geophysical and lithological features characterise the NW and SE parts of the area compared to the central region. The NW and SE parts predominantly comprise medium-grade garnet-kyanite gneiss, which exhibits higher gamma intensities than the central region, dominated by low-grade rocks and low gamma intensities (Figure 8 b). According to Kondor & M. Tóth (2021), these three blocks were probably juxtaposed along post-metamorphic normal faults during the Miocene syn-rift extensional processes, although they may also reflect different nappe units. However, based on the geophysical interpretation, the three main blocks can be well-defined, but the two low-grade blocks cannot be distinguished based on their gamma intensities. The postmetamorphic normal fault between them can only be inferred based on their petrological characteristics.

Lithological characteristics of the SE part of AH

The 3D model of the entire area revealed an anomaly with exceptionally high gamma intensities in the SE part of the AH area (*Figure 4*). Focusing on this part, the refined 3D block model highlights additional wells with higher gamma

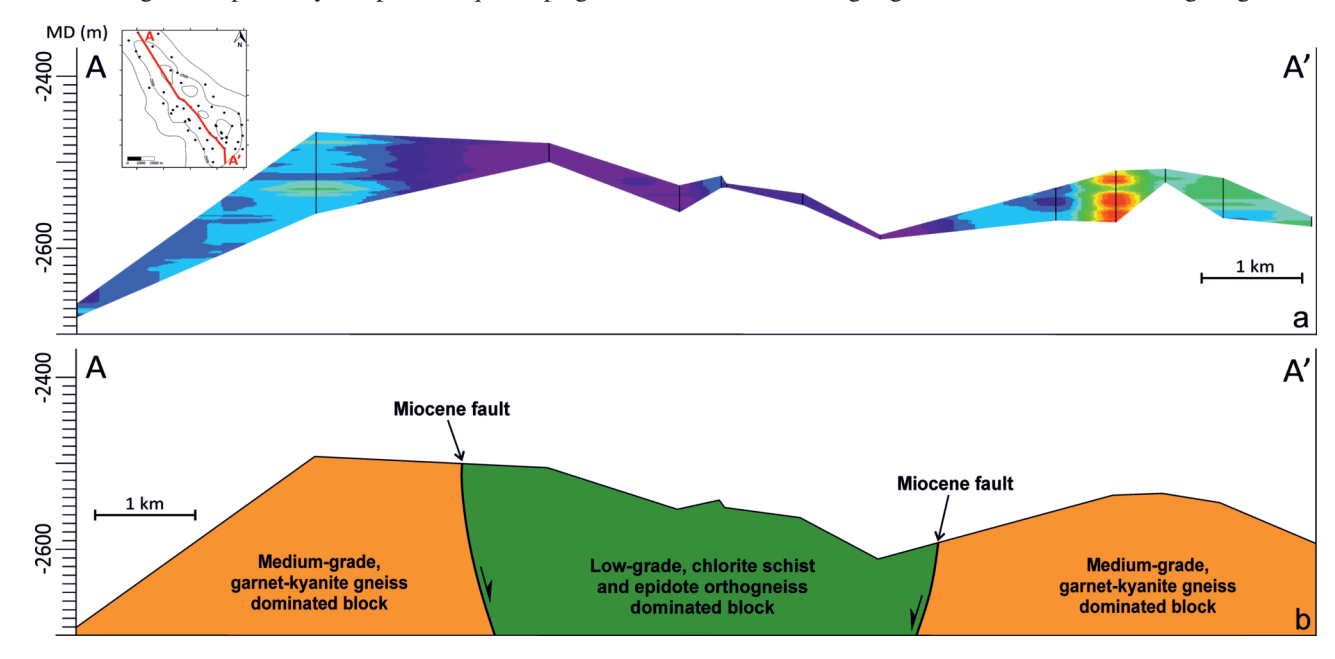


Figure 8. NW–SE cross-section of the Algyő High region. a) Cross-section across the Algyő High displaying the distribution of natural gamma-ray intensity (NGR) values [Conditional Gamma Units (CGU)]. Black lines indicate the locations of boreholes. The point map of the area illustrates the A-A' cross-sections line and the wells with NGR [CGU] data. MD: measured depth. b) Geological interpretation of the natural gamma-ray intensity in conjunction with the previous petrological interpretation by Kondor & M. Tóth (2021). The vertical scale of the cross-sections is exaggerated 2×.

8. ábra. Az Algyő-hát ÉNy-DK irányú szelvénye. a) A természetes gamma intenzitás (natural gamma-ray intensity: NGR) [Feltételes Gamma Egység (Conditional Gamma Units: CGU)] értékek eloszlását mutató szelvény. A fekete vonalak a fúrások helyét jelölik. A terület ponttérképe az A-A' szelvények nyomvonalát és az adatokat szolgáltató fúrási pontok helyét jelöli. Az 'MD: measured depth' a mért mélységet jelöli. b) A természetes gamma intenzitás-értékek földtani értelmezése, figyelembe véve KONDOR & M. Tóth (2021) korábbi kőzettani értelmezését. A szelvények függőleges méretaránya kétszeres nagyítású.

intensities than the average (Figure 6). A detailed petrographic analysis was conducted to understand the NGR characteristics of this sub-area. The analysis identified three different rock types with unique mineralogical compositions: garnet-kyanite gneiss, garnetiferous amphibolite and metagranite. The most common lithology is garnet-kyanite gneiss. According to previous publications, this gneiss mass was affected by polyphase metamorphism (SZALAY 1977; SZEDER-KÉNYI 1984; T. KOVÁCS & KURUCZ 1984; HORVÁTH & ÁRKAI 2002; Lelkes-Felvári et al. 2003, 2005; Kondor & M. Tóth 2021). The first, amphibolite facies regional metamorphic event, is represented by relic biotite and muscovite flakes, large garnet porphyroblasts, and rutile grains. The second event is characterised by fine-grained kyanite aggregates replacing garnet porphyroblasts. KONDOR & M. TÓTH (2021) proposed that the second event was a contact metamorphic (metasomatic) process associated with an igneous intrusion, which may have also resulted in tourmaline crystallisation. Garnetiferous amphibolite has been identified only in a few core samples. Peak metamorphic conditions are defined by rock-forming green or dark brown amphibole crystals, inclusion-rich garnet porphyroblasts, and rutile grains. The presence of this mineral assemblage suggests peak conditions corresponding to the middle amphibolite facies. Although mineralogical compositions and protoliths of the garnet-kyanite gneiss and garnetiferous amphibolite are different, these rock types evolved simultaneously under peak amphibolite facies metamorphic conditions (KONDOR & M. TOTH 2021). The petrographic features and the qualitative metamorphic evolution of the metagranite significantly differ from those of the garnet-kyanite gneiss and garnetiferous amphibolite. The rock-forming minerals and accessories represent the minerals of the protolith, while purely metamorphic minerals were not found. Microtextural features of the metagranite, such as the presence of microcline, idiomorphic zircon crystals, myrmekitic plagioclase feldspars, and crystals with polygonal microtextures, all indicate the intrusive, magmatic origin of the rocks (VERNON & COLLINS 1988).

Correlation of lithology and NGR values in the SE part of the AH area

As previously demonstrated, the NGR log is quite sensitive to the mineralogical and chemical composition of rocks. Radioactivity is primarily emitted from potassium, thorium, and uranium. Accordingly, potassium-bearing minerals, such as K-feldspar, biotite, and muscovite, as well as uranium-bearing minerals, such as zircon, can increase the gamma-ray intensity of the rocks. In contrast, the absence or small amounts of these minerals can reduce gamma radiation. Consequently, the NGR values observed in the boreholes serve as reliable indicators of the chemical and mineralogical composition of the surrounding rock mass, thus allowing the geophysical—lithological correlation.

The three main rock types in the SE part of the AH area are characterised by distinct mineralogical compositions.

The main mineral phases in the garnet-kyanite gneiss are biotite, muscovite, quartz, and K-feldspar, while amphibolite is dominated by amphibole, plagioclase and garnet. Metagranite primarily comprises K-feldspar and quartz, with subordinate plagioclase feldspar and muscovite, and contains a minor amount of biotite. Regarding the primary composition of the garnet-kyanite gneiss, the main source of gamma radiation are the micas with a secondary contribution from feldspars. In the garnetiferous amphibolite, the gamma radiation essentially depends on a small amount of biotite. In metagranite, gamma radiation primarily originates from the dominant K-feldspar, with a secondary contribution from the mica content. Additionally, as an accessory phase, zircon may contribute to the gamma radiation of metagranite. Considering the mineralogical composition of these rock types, the highest gamma intensity is expected in boreholes intersecting metagranite. In contrast, the lowest gamma intensity is likely to occur in garnetiferous amphibolite. The gamma intensity is expected to range between the highest and lowest values for garnet-kyanite gneiss.

Based on petrographic analyses of core samples, garnetkyanite gneiss is present in most boreholes. The typical gamma intensities in these boreholes range from 10 to 14 CGU (Figure 6). However, zones with higher gamma intensities (14-18 CGU), as observed in Well-6, can also be found inside the gneiss mass. A core sample from the upper part of Well-6 (-2492 to -2500 metres) revealed garnetkyanite gneiss, associated with a nearly consistent gamma intensity of 14-16 CGU. Between depths of -2510 and -2533 metres, the gamma intensity decreases to 6–10 CGU, corresponding to core samples identified as garnetiferous amphibolite. Subsequently, the well-log shows higher CGU values (14-18 CGU), similar to those in the upper zone (Figure 6). Core samples from the lower zone also revealed garnet-kyanite gneiss. In Well-2, although the upper zone shows slightly lower gamma values (14-18 CGU), an increase is observed in the bottom section (18-22 CGU) (Fig*ure* 6). Core sampling consistently revealed the entire rock column as metagranite; however, there is a slight variation in the CGU range. Similarly, higher values (18–22 CGU) are observed in other boreholes, such as Well-1 and Well-7, where the positive anomaly can also be associated with metagranite.

The typical gamma-ray intensities of garnet-kyanite gneiss range from 10 to 14 CGU, while those of metagranite generally vary between 18 and 22 CGU. However, intermediate gamma values (14–18 CGU) are also observed within the garnet-kyanite gneiss and metagranite units, leading to uncertainties in lithological identification based on CGU values alone. In boreholes that intersect metagranite, lower CGU values are often recorded in the upper sections of the rock column. These reduced values (16–18 CGU) may indicate a weathered top zone of the metamorphic basement. Low-temperature alteration processes, such as K-feldspar sericitisation and potassium leaching due to its mobile behaviour, can decrease the K-content, resulting in reduced gamma values.

Conversely, the higher gamma values (14-18 CGU) observed in garnet-kyanite gneiss adjacent to granite-dominated zones (Figure 6) may be attributed to a different mechanism. Changes in natural gamma-ray intensity can reflect metasomatic or hydrothermal alterations in metamorphic rocks (BARTETZKO et al. 2005). This effect is most pronounced in boreholes intersecting garnet-kyanite gneiss to the southeast and east of Well-4 (e.g., Well-6). In contrast, in boreholes to the northeast and west, these elevated values were not observed. Elevated gamma intensities typically indicate increased Kcontent, often associated with potassium metasomatism. Such metasomatising fluids usually originate from magmatic or low-temperature aqueous systems (Ennis et al. 2000). In this context, the subareas with 14-18 CGU values within garnetkyanite gneiss-dominated zones are interpreted as metasomatised regions. The close spatial association between these zones suggests that the metasomatic overprint likely resulted from the granitoid magmatism itself.

Gamma intensities in Well-4 are exceptionally high, ranging from 22 to 31 CGU, suggesting the presence of metagranite (*Figure 6*). Nevertheless, the specific chemical anomaly responsible for these elevated intensities remains unclear in the absence of spectral gamma-ray measurements. While potassium significantly contributes to gamma radiation, uranium and thorium can also play a role. The concentrations of these radioactive elements are primarily determined by the mineralogical composition but can be modified by post-magmatic processes. Metasomatic alteration due to hydrothermal activity can modify the concentration and distribution of radioactive elements within the formations, thereby influencing gamma radiation levels (BARTETZKO et al. 2000, Luo & Heping 2010).

In the vicinity of granite intrusions, hydrothermal fluids can increase gamma intensities in the surrounding host rocks and also inside the granitoid body (ZIELINSKI & MEIER 1988). Thorium, being relatively insoluble, contributes less to these enhancements (CSÓKÁS 1993). In contrast, as a mobile element, uranium can be readily transported by hydrothermal or subsurface waters and accumulate, particularly in veins. Since uranium has a significantly higher gamma radiation output per unit weight than potassium (CSÓKÁS 1993), its enrichment could markedly increase gamma intensity. Therefore, the elevated gamma values observed in Well-4 may be attributed to metasomatic and hydrothermal processes that affected the formation. So, the borehole is interpreted as hydrothermally altered metagranite.

The core samples in Well-6 and Well-5 revealed garnetiferous amphibolite associated with lower gamma intensities ranging from 6–10 CGU (*Figure 6*). A similar zone with low values was recognised in an additional borehole (Well-3), which is also assumed to be garnetiferous amphibolite.

Based on the petrographic correlation of the well-logs, the rock types in all boreholes were identified by considerű composition (*Figure 9*). As a result, the observed gamma intensities indicate that metagranite is associated with the highest values, whereas the lowest values characterise garnetiferous amphibolite. Although the gamma intensities of

garnet-kyanite gneiss are higher than those of amphibolite but lower than those of metagranite, zones with higher gamma intensities were also identified inside the gneiss mass, which were interpreted as metasomatised gneiss.

After re-evaluation, histogram analyses were conducted for the identified rock types, providing statistical data for their distinct characteristics (Figure 10). The largest population characterises the garnet-kyanite gneiss. It exhibits a mean natural gamma-ray intensity of 12 CGU, ranging from 9 to 14 CGU, aligning closely with typical observed values of 10-14 CGU. In contrast, garnetiferous amphibolite shows the lowest NGR values, ranging from 6 to 11 CGU, with a mean of 9 CGU. The metasomatised gneiss represents the transition between garnet-kvanite gneiss and metagranite. and it is associated with a mean NGR value of 16 CGU, ranging from 13 to 19 CGU. Gamma values of 16-18 CGU primarily represent the weathered top zone of metagranite. The metagranite has the highest NGR values, ranging from 16 to 22 CGU, and it has the smallest population, with a mean NGR value of 19 CGU. The values detected in Well-4 are presented separately and identified as hydrothermally altered metagranite. This borehole is characterised by outlier NGR values, with a wide range and high variability. The mean NGR value of this population is 27 CGU in the 20–32 range.

Spatial correlation

The compiled geological cross-sections represent the spatial distribution of the primary lithologies (*Figure 11*). Based on the geophysical–lithological correlation, in addition to the main lithotypes – garnet–kyanite gneiss, metagranite, and amphibolite – a new rock type, metasomatised gneiss, has been distinguished. The garnet–kyanite gneiss dominates the SE part of the AH area, intercalated by garnetiferous amphibolite in some boreholes in narrow zones. Kondor & M. Tóth (2021) proposed that the garnetiferous amphibolite represents mafic magmatic dykes that crosscut the host gneiss body and that both rock types underwent comparable metamorphic evolution.

Metagranite is an intrusive igneous granitoid rock identified in several boreholes in well-defined areas. Previous studies have also described young granite bodies intruding the gneiss and mica schist formations in the SE part of AH (SZALAY 1977, T. KOVÁCS & KURUCZ 1984, SZEDERKÉNYI 1984). SZEDERKÉNYI (1984) suggested that these intrusions are linked to the Late Cretaceous 'banatite' magmatism that affected the entire region. Considering the petrographic features and the metamorphic evolution of the garnet-kyanite gneiss and metagranite, in conjunction with previous interpretations, the metagranite can be interpreted as younger granitoid dykes that penetrated the gneiss mass. A large granite body related to 'banatite' magmatism has been documented to the south of AH in the Ferencszállás area (SZEDERKÉNYI 1984, T. KOVÁCS & KURUCZ 1984). The metagranite bodies locally occurring within the garnet-kyanite gneiss are likely related to this large-scale granitoid intrusion.

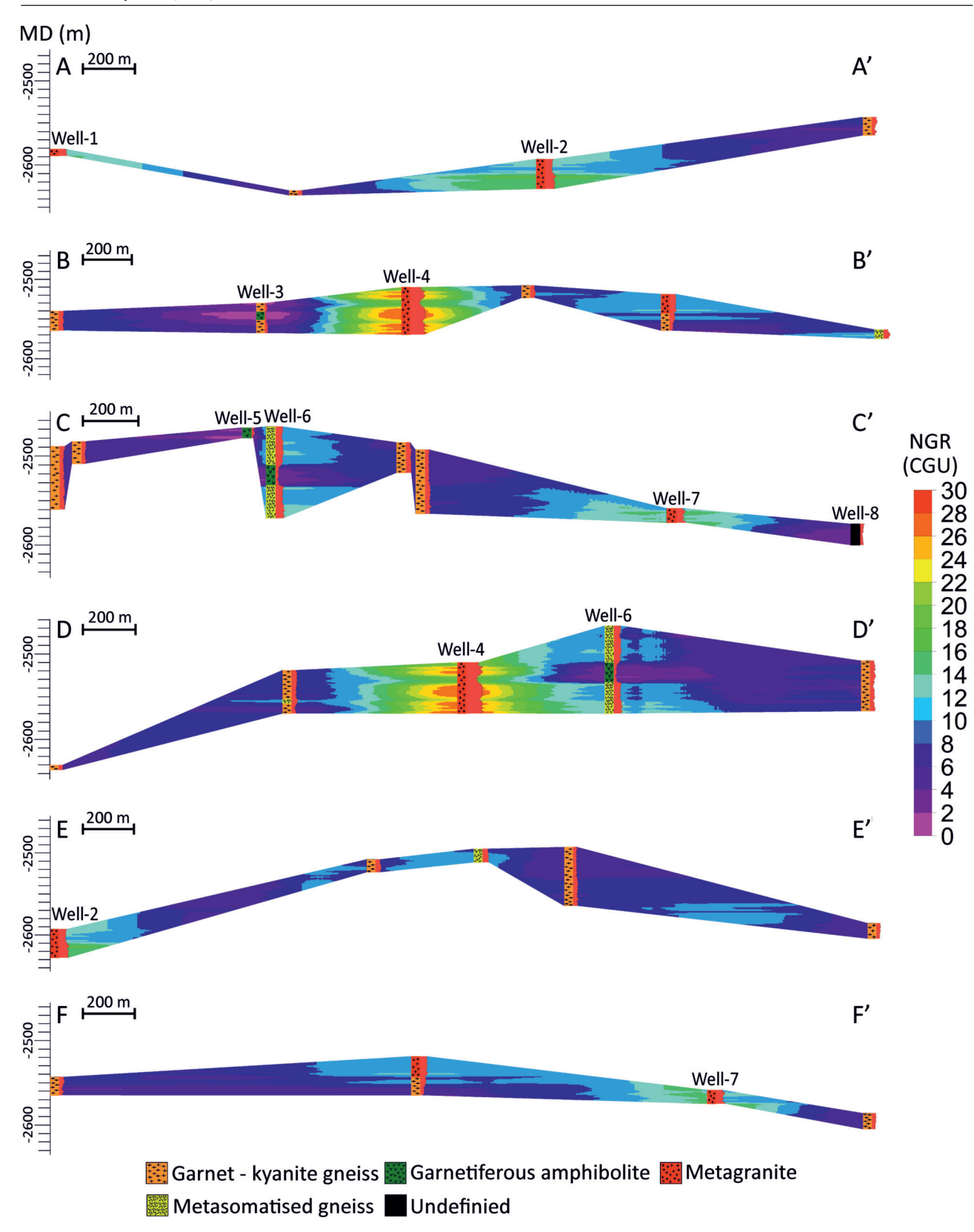


Figure 9. Reinterpreted cross-sections across the SE part of Algyő High showing the distribution of natural gamma-ray intensity (NGR) [Conditional Gamma Units (CGU)] values. The rock types in all boreholes were identified by considering typical CGU values. The vertical scale of the cross-sections is exaggerated $2\times$. MD: measured depth

9. ábra. Az Algyő-hát DK-i területén mélyült fúrásokban mért természetes gamma intenzitás (natural gamma-ray intensity: NGR) [Feltételes Gamma Egység (Conditional Gamma Units: CGU] értékeinek eloszlását ábrázoló újraértelmezett szelvények. A jellemző Feltételes Gamma Egység (CGU) értékei alapján minden fúrásban azonosításra kerültek a fő kőzettípusok. A szelvények függőleges méretaránya kétszeres nagyítású. Az 'MD: measured depth' a mért mélységet jelöli

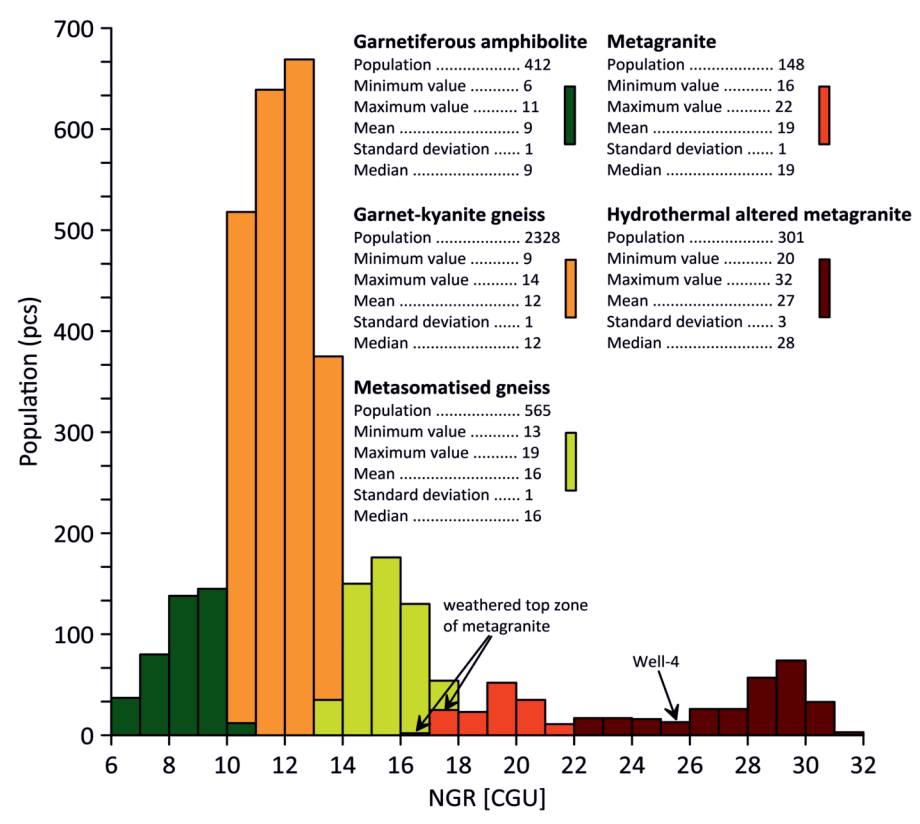


Figure 10. Statistical evaluation of the natural gamma-ray intensity (NGR) [Conditional Gamma Units (CGU)] characterising the main rock types of the SE part of Algyő High

10. ábra. Az Algyő-hát DK-i részének fő kőzettípusait jellemző természetes gamma intenzitásának (natural gamma-ray intensity: NGR) [Feltételes Gamma Egység (Conditional Gamma Units: CGU] statisztikai értékelése

These granitoid bodies in the area have likely influenced the mineralogical and chemical composition of the surrounding host gneiss. Hydrothermal fluids associated with these intrusions may have metasomatised the host rock and remobilised certain elements. As previously discussed, the zones with increased gamma intensities observed in the garnet–kyanite gneiss are likely the result of metasomatic processes linked to these granitoid intrusions. These zones, which primarily occur in the surroundings of the metagranite bodies, have been identified as metasomatised gneiss (*Figure 11*).

Conclusion

Over the past few decades, several boreholes have penetrated the crystalline basement of the Algyő High (AH) region, yielding substantial core samples and well-log data. This study re-evaluates the crystalline basement using an integrated approach that combines well-log interpretation, core analysis, and petrographic observations.

Among the available wireline logs, natural gamma-ray intensity [CGU] logs proved to be the most suitable for geophysical—lithological correlation in this area.

Based on the NGR [CGU] log data, the AH metamorphic basement comprises three major blocks, consistent with earlier petrological studies. Higher gamma-ray intensities (8–16 CGU) were recorded in the NW and SE parts, which are predominantly composed of medium-grade garnet–ky-

anite gneiss, while the central region is dominated by low-grade lithologies showing lower gamma-ray values (2–8 CGU).

Gamma-ray anomalies were identified in the SE part of the area. Petrographic analysis of core samples and thin sections revealed three principal rock types in this region: garnet-kyanite gneiss, garnetiferous amphibolite, and metagranite.

Geophysical–lithological correlations show that garnet–kyanite gneiss is the dominant rock type in the SE block, with typical gamma-ray intensities of 10–14 CGU. This gneiss mass is intercalated with garnetiferous amphibolite characterised by lower values (6–10 CGU).

The metagranite exhibits the higher gamma-ray intensities (18–22 CGU) and is interpreted as representing younger granite/granodiorite intrusive dykes within the host gneiss. These magmatic bodies locally altered the mineralogical and chemical composition of the gneiss, producing metasomatised zones.

The results highlight the importance of integrating geophysical and lithological data to improve understanding of the complex structure and metamorphic evolution of the AH basement.

As existing wells reached only the uppermost part of the metamorphic basement, current interpretations are limited to lateral structures, with deeper levels remaining unexplored. To address this limitation, the incorporation of reflection seismic data is recommended.

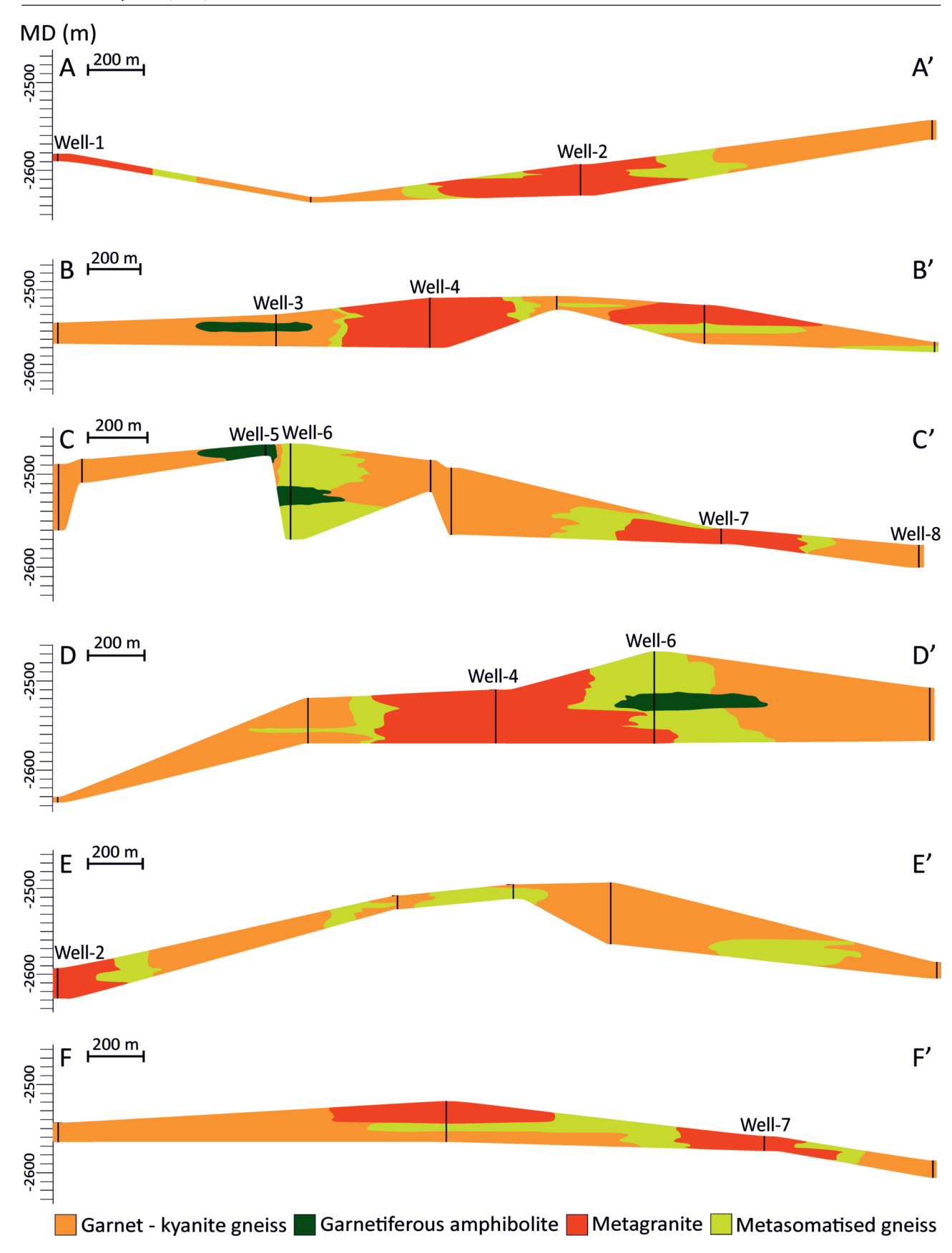


Figure 11. Geological cross-sections representing the spatial distribution of the main rock types based on geophysical-lithological correlation. The vertical scale of the cross-sections is exaggerated $2\times$. MD: measured depth

11. ábra. A geofizikai-kőzettani korreláció alapján meghatározott fő kőzettípusok térbeli eloszlását mutató geológiai szelvények. A szelvények függőleges méretaránya kétszeres nagyítású. Az 'MD: measured depth' a mért mélységet jelöli

Acknowledgement

The MOL Hungarian Oil and Gas Company is thanked for providing thin sections, core samples, and wireline logs for investigation. We are grateful to Gábor TARI, Wolfgang

HUJER, and an anonymous reviewer for their constructive comments on the manuscript. This research was funded by the National Research, Development and Innovation Office, grant number K-138919.

References - Irodalom

- BALOGH, K. & PÉCSKAY, Z. 2001: K/Ar and Ar/Ar geochronological studies in the PANCARDI region. *Acta Geologica Hungarica* 44/2–3, 281–299.
- Bartetzko, A., Delius, H. & Pechnig, R. 2005: Effect of compositional and structural variations on log responses of igneous and metamorphic rocks. I: mafic rocks. *Geological Society, London, Special Publications* **240**, 255–278. https://doi.org/10.1144/GSL.SP.2005.240.01.19
- BERZA, T., CONSTANTINESCU, E. & VLAD, S. 1998: Upper Cretaceous magmatic series and associated mineralization in the Carpathian-Balkan orogen. *Resource Geology* **48**, 291–306. https://doi.org/10.1111/j.1751-3928.1998.tb00026.x
- Csókás J. 1993: Mélyfúrási geofizika. Nemzeti Tankönyvkiadó, Budapest.
- CSONTOS, L. & VÖRÖS, A. 2004: Mesozoic plate tectonic reconstruction of the Carpathian region. *Palaeogeography, Palaeoclimatology, Palaeoecology* **210**, 1–56. https://doi.org/10.1016/j.palaeo.2004.02.033
- CSONTOS, L., NAGYMAROSY, A., HORVÁTH, F. & KOVÁČ, M. 1992: Cenozoic evolution of the Intra-Carpathian area: A model. *Tectonophysics* 208/1–3, 221–241. https://doi.org/10.1016/0040-1951(92)90346-8
- ENNIS, D. J., DUNBAR, N. W., CAMPBELL, A. R. & CHAPIN, C. E. 2000: The effects of K-metasomatism on the mineralogy and geochemistry of silicic ignimbrites near Socorro, New Mexico. Chemical Geology 167, 285–312. https://doi.org/10.1016/S0009-2541(99)00223-5
- FISER-NAGY, Á., VARGÁNÉ TÓTH, I. & M. TÓTH, T. 2014: Lithology identification using open-hole well-log data in the metamorphic Kiskunhalas-NE hydrocarbon reservoir, South Hungary. *Acta Geodaetica et Geophysica Hungarica* **49/1**, 57–78. https://doi.org/10.1007/s40328-013-0037-1
- HAAS, J. 2001: Geology of Hungary. Eötvös University Press, Budapest.
- HAAS, J., BUDAI, T., CSONTOS, L., FODOR, L. & KONRÁD, GY. 2010: Pre-Cenozoic Geological Map of Hungary 1:500 000. Hungarian Geological Institute. https://map.mbfsz.gov.hu/preterc500/
- HASAN, M. L. & M. TÓTH, T. 2023: Localization of potential migration pathways inside a fractured metamorphic hydrocarbon reservoir using well log evaluation (Mezősas field, Pannonian Basin). *Geoenergy Science and Engineering* **225/24**, 211710. https://doi.org/10.1016/j.geoen.2023.211710
- HORVÁTH, F. & TARI, G. 1999: IBS Pannonian Basin project: a review of the main results and their bearings on hydrocarbon exploration. The Mediterranean basins: Tertiary extension within the Alpine orogene. *Geological Society, London, Special Publication* **156**, 195–213. https://doi.org/10.1144/gsl.sp.1999.156.01.11
- HORVÁT, P. & ÁRKAI, P. 2002: Pressure-temperature path of metapelites from the Algyő–Ferencszállás area, SE Hungary: thermobaro-metric constraints from coexisting mineral assemblages and garnet zoning. Acta Geologica Hungarica 45/1, 1–27. https://doi.org/10.1556/ageol.45.2002.1.1
- JUHÁSZ Á. 1969: A Duna–Tisza köze mélységi magmás és metamorf képződményei. Földtani Közlöny 99, 320–336.
- KONDOR, H. & M. TÓTH, T. 2021: Contrasting metamorphic and post-metamorphic evolutions within the Algyő basement high (Tisza Mega-unit, SE Hungary). Consequences on structural history. Central European Geology 64/2, 91–112. https://doi.org/10.1556/24.2021.00004
- LARSEN, E. S., Jr., & PHAIR, G. 1954: The distribution of uranium and thorium in igneous rocks. In: *Nuclear Geology*. J. Wiley & Sons, New York, 75–89.
- Lelkes-Felvári, Gy., Frank, W. & Schuster, R. 2003: Geochronological constraints of the Variscan, Permian-Triassic and eo-Alpine (Cretaceous) evolution of the Great Hungarian Plain basement. *Geologica Carpathica* **54**, 267–280.
- Lelkes-Felvári, Gy., Schuster, R., Frank, W. & Sassi, R. 2005: Metamorphic history of the Algyő High (Tisza Mega-unit, basement of Great Hungarian Plain) a counterpart of crystalline units of the Koralpe-Wölz nappe system (Austroalpine, Eastern Alps). *Acta Geologica Hungarica* 48, 371–394. https://doi.org/10.1556/ageol.48.2005.4.2
- Luo, M. & Pan, H. 2010: Well Logging Responses of UHP Metamorphic Rocks from CCSD Main Hole in Sulu Terrane, Eastern Central China. *Journal of Earth Science* 21/3, 347–357. https://doi.org/10.1007/s12583-010-0098-9
- М. Тотн Т. 2008: Repedezett, metamorf fluidumtárolók az Alföld aljzatában. МТА doktori értekezés, Szeged.
- М. То́тн, Т. & VARGÁNÉ Tóтн, I. 2020: Lithologically controlled behaviour of the Dorozsma metamorphic hydrocarbon reservoir (Pannonian Basin, SE Hungary). – Journal of Petrol Science and Engineering 195, 107748. https://doi.org/10.1016/j.petrol.2020.107748
- M. То́тн, T., Fiser-Nagy, Á., Kondor, H., Molnár, L., Schubert, F., Vargáné Tóтн, I. & Zachar, J. 2021: Az Alföld metamorf aljzata: a köztes tömegtől a tarka mozaikig. Földtani Közlöny 151/1, 3–26. https://doi.org/10.23928/foldt.kozl.2021.151.1.3

MAGYAR, I., FOGARASI, A., VAKARCS, G., BUKÓ, L. & TARI, G. 2006: The largest hydrocarbon field discovered to date in Hungary: Algyő. – In: Golonka, J. & Picha, F. (eds): *The Carpathians and their Foreland: Geology and Hydrocarbon Resources: AAPG Memoir* **84**, 619–632. https://doi.org/10.1306/985734M843142

- MOLNÁR, L., M. TÓTH, T. & SCHUBERT, F. 2015: Structural controls on the petroleum migration and entrapment within faulted basement blocks of the Szeghalom Dome (Pannonian Basin, SE Hungary). *Geologia Croatica* **68/3**, 247–259. https://doi.org/10.4154/GC.2015.19
- NAGY, Á., M. TÓTH, T., VÁSÁRHELYI, B. & FÖLDES, T. 2013: Integrated core study of a fractured metamorphic HC-reservoir; Kiskunhalas-NE, Pannonian Basin. *Acta Geodaetica et Geophysical* **48/1**, 53–75. https://doi.org/10.1007/s40328-012-0008-y
- Neubauer F. 2002: Contrasting Late Cretaceous to Neogene ore provinces in the Alpine–Balkan–Carpathian–Dinaride collision belt. The Timing and Location of Major Ore Deposits in an Evolving Orogen. *Geological Society, London, Special Publications* **204**, 81–202. https://doi.org/10.1144/GSL.SP.2002.204.01.06
- PECHNIG, R., DELIUS, H. & BARTETZKO, A. 2005: Effect of compositional and structural variations on log responses of igneous and metamorphic rocks. II: acid and intermediate rocks. *Geological Society, London, Special Publications* **240**, 279–300. https://doi.org/10.1144/GSL.SP.2005.240.01.20
- Posgay, K., Takács, E., Szalai, I., Bodoky, T., Hegedús, E., Jánváriné, K. I., Tímár, Z., Varga, G., Bérczi, I. & Szalay, Á. 1996: International deep reflection survey along the Hungarian Geotraverse. *Geophysical Transactions* 40/1–2, 1–44.
- REISER M. K. 2015: The tectonometamorphic evolution of the Apuseni Mountains during the Cretaceous, Investigation on the interplay between tectonics and surface processes in the build-up of a source area. Dissertation, University of Innsbruck.
- RUMPLER, J. & HORVÁTH, F. 1988: Some representative seismic reflection lines from the Pannonian basin and their structural interpretation. The Pannonian basin A study in basin evolution. AAPG, Memoir 45, 53–169. https://doi.org/10.1306/M45474C13
- SCHMID, S. M., BERNOULLI, D., FÜGENSCHUH, B., MATENCO, L., SCHEFER, S., SCHUSTER, R., TISCHLER, M. & USTASZEWSKI, K. 2008: The Alpine-Carpathian-Dinaridic orogenic system: correlation and evolution of tectonic units. *Swiss Journal of Geosciences* 101, 139–183. https://doi.org/10.1007/s00015-008-1247-3
- SCHUBERT, F., DIAMOND, L. W. & M. TÓTH, T. 2007: Fluid-inclusion evidence of petroleum migration through a buried metamorphic dome in the Pannonian Basin, Hungary. *Chemical Geology* **244**, 357–381. https://doi.org/10.1016/j.chemgeo.2007.05.019
- SERRA, O. 1984: Fundamentals of Well-Log Interpretation. Developments in Petroleum Science, 15A, Elsevier, Amsterdam.
- SZALAY, Á. 1977: Metamorphic-granitogenic rocks of the basement complex of the Great Hungarian Plain, Eastern Hungary. *Acta Mineralogica-Petrographica* **23/1**, 49–69.
- SZEDERKÉNYI T. 1984: Az Alföld kristályos aljzata és földtani kapcsolatai. MTA doktori értekezés, Szeged.
- T. Kovács, G. & Kurucz, B. 1984: A Dél-Alföld mezozoikumnál idősebb képződményei. Magyar Állami Földtani Intézet, Budapest, 15–19. Tari, G. 1996: Extreme crustal extension in the Rába River extensional corridor (Austria/Hungary). – Mitteilungen der Gesellschaft der Geologie- und Bergbaustudenten in Österreich 41, 1–17.
- Tari, G., Horváth, F. & Rumpler, J. 1992: Styles of extension in the Pannonian Basin. *Tectonophysics* **208**, 203–219. https://doi.org/10.1016/0040-1951(92)90345-7
- Tari, G., Dövényi, P., Dunkl, I., Horváth, F., Lenkey, L., Stefanescu, M., Szafián, P. & Tóth, T. 1999: Lithospheric structure of the Pannonian Basin derived from seismic, gravity and geothermal data. The Mediterranean basins: Tertiary extension within the Alpine orogene. *Geological Society, London, Special Publication* 156, 215–250. https://doi.org/10.1144/GSL.SP.1999.156.01.12
- Tari, G., Bada, G., Boote, D., Krézsek, Cs., Koroknai, B., Kovács, G., Lemberkovics, V., Sachsenhofer, R. & Tóth, T. 2003: The Pannonian Super Basin: A brief overview. AAPG Bulletin 107/8, 1391–1417. https://doi.org/10.1306/02172322098
- VERNON, R. H. & COLLINS, W. J. 1988: Igneous microstructures in migmatites. Geology 16, 1126–1129. https://doi.org/10.1130/0091-7613(1988)016<1126:IMIM>2.3.CO;2
- WHITNEY, D. L. & EVANS, B. W. 2010: Abbreviations for names of rock-forming minerals. *American Mineralogist* 95, 185–187. https://doi.org/10.2138/am.2010.3371
- ZIELINSKI, R. & MEIER, A. 1988: The association of uranium with organic matter in Holocene peat: An experimental leaching study. *Environmental Science* 3/6, 631–643. https://doi.org/10.1016/0883-2927(88)90095-9
- ZIMMERMAN, A., STEIN, H. J., HANNAH, J. L., KOŽELJ, D., BOGDANOV, K. & BERZA, T. 2008: Tectonic configuration of the Apuseni-Banat-Timok-Srednogorie belt, Balkans-South Carpathians, constrained by high precision Fe-Os molybdenite ages. *Mineralium Deposita* 43, 1–21. https://doi.org/10.1007/s00126-007-0149-z

Manuscript received: 24.03.2025.